

Lymphoid follicle destruction and immunosuppression after repeated CpG oligodeoxynucleotide administration

Mathias Heikenwalder^{1,5}, Magdalini Polymenidou^{1,5}, Tobias Junt², Christina Sigurdson¹, Hermann Wagner³, Shizuo Akira⁴, Rolf Zinkernagel² & Adriano Aguzzi¹

DNA containing unmethylated cytidyl guanosyl (CpG) sequences, which are underrepresented in mammalian genomes but prevalent in prokaryotes, is endocytosed by cells of the innate immune system, including macrophages, monocytes and dendritic cells¹, and activates a pathway involving Toll-like receptor-9 (TLR9)². CpG-containing oligodeoxynucleotides (CpG-ODN) are potent stimulators of innate immunity, and are currently being tested as adjuvants of antimicrobial, antiallergic, anticancer and antiprion immunotherapy. Little is known, however, about the consequences of repeated CpG-ODN administration, which is advocated for some of these applications. Here we report that daily injection of 60 µg CpG-ODN dramatically alters the morphology and functionality of mouse lymphoid organs. By day 7, lymphoid follicles were poorly defined; follicular dendritic cells (FDC) and germinal center B lymphocytes were suppressed. Accordingly, CpG-ODN treatment for ≥7 d strongly reduced primary humoral immune responses and immunoglobulin class switching. By day 20, mice developed multifocal liver necrosis and hemorrhagic ascites. All untoward effects were strictly dependent on CpG and TLR9, as neither the CpG-ODN treatment of *Tlr9*^{-/-} mice nor the repetitive challenge of wild-type mice with nonstimulatory ODN (AT-ODN) or with the TLR3 agonist polyinosinic:cytidylic acid (polyI:C) were immunotoxic or hepatotoxic.

CpG-ODN, when applied repetitively, exert a protective effect on mice inoculated with scrapie prions³. This was unexpected because B lymphocytes⁴ and dendritic cells⁵, which are expanded by exposure to CpG-ODN, are involved in prion neuroinvasion. In addition, *Myd88*^{-/-} mice, in which TLR9 signaling is impaired^{6,7}, show unaltered prion susceptibility⁸. Because lymphoid germinal centers are crucial to peripheral prion pathogenesis^{9,10}, we studied the effects of CpG-ODN (1826) on the microarchitecture and function of mouse secondary lymphoid organs.

C57BL/6 mice were treated for 2–20 d with CpG-ODN, non-stimulatory AT-ODN or PBS, and killed 24 h after the last injection.

Splenic follicles appeared subtly altered after just 2 d of CpG-ODN treatment (data not shown). After 7 d, spleen weight in CpG-ODN-treated mice increased approximately fivefold compared with AT-ODN- and PBS-treated mice^{11,12} (Fig. 1). Mesenteric lymph nodes and inguinal lymph nodes were hyperplastic in CpG-ODN-treated wild-type mice (Fig. 2). Splenomegaly was mainly due to erythroid and myeloid expansion in the red pulp¹¹. Follicle microarchitecture in spleen, mesenteric lymph nodes and inguinal lymph nodes was severely disturbed. B-cell follicles were enlarged (Fig. 1a), possibly because of plasma cell expansion¹¹. CD21⁺CD35⁺IgM⁺IgD⁻ marginal zone B lymphocytes were strongly reduced, and MOMA-1⁺ metallophilic marginal zone macrophage festoons and MOMA-1⁺ rings of metallophilic marginal zone macrophages were loosened (Fig. 1a and Supplementary Fig. 1 online). CD4⁺ and CD8⁺ T-cell zones were somewhat enlarged (Supplementary Fig. 1 online). Compared with AT-ODN-treated mice, numbers of splenic white-pulp follicles were reduced four- to fivefold, and FDC-M1⁺ networks and peanut agglutinin (PNA)⁺ clusters were reduced six- to sevenfold (Fig. 1c).

After 14 d of CpG-ODN treatment, disruption of lymphoid microarchitecture had progressed further. Total cellularity was increased 20-fold in spleen and 2-fold in mesenteric lymph nodes (Fig. 2b). Follicles were replaced by disorganized B-lymphocyte collections with few scattered FDC-M1⁺ cells. PNA⁺ clusters were virtually abolished. Marginal zones were severely disorganized (data not shown).

After 20 d, splenic microarchitecture was even further compromised (Fig. 1a,b). Marginal zone B lymphocytes were no longer detectable, and MOMA-1⁺ cells were strongly reduced (Fig. 1a). CD8⁺ and CD4⁺ T-cell zones were disorganized (Fig. 1b and data not shown). In contrast, CpG-ODN-treated *Tlr9*^{-/-} and AT-ODN-treated wild-type spleens² were unremarkable after 20 d of treatment (Fig. 1a,b).

Splenomegaly (Fig. 2a,b), in CpG-ODN-treated mice (≥14 d) was caused mostly by a prominent expansion of erythroid and myeloid lineages (data not shown). Accordingly, the prevalence of macrophages and dendritic cells was unchanged (Fig. 2c), whereas

¹Institute of Neuropathology and ²Institute of Experimental Immunology, University Hospital of Zürich, Schmelzbergstrasse 12, CH-8091 Zürich, Switzerland.

³Institute for Medical Microbiology, Immunology and Hygiene, University of Munich, Trogerstrasse 9, D-81675 Munich, Germany. ⁴Department of Host Defense, Research Institute for Microbiological Diseases, Osaka University, 3-1 Yamada-oka, Suita, Osaka 565-0871, Japan. ⁵These authors contributed equally to this work. Correspondence should be addressed to A.A. (adriano@pathol.unizh.ch).

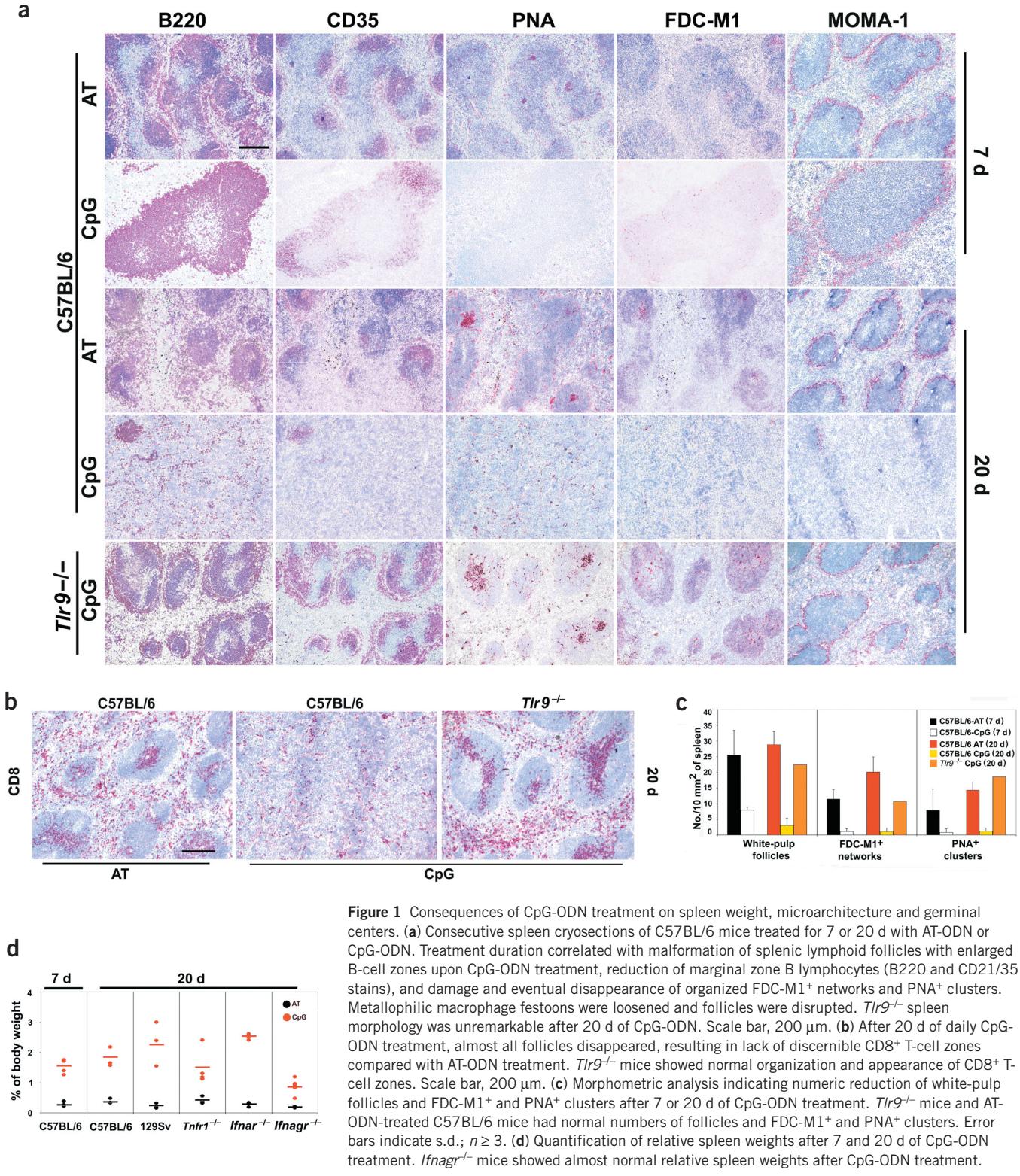


Figure 1 Consequences of CpG-ODN treatment on spleen weight, microarchitecture and germinal centers. **(a)** Consecutive spleen cryosections of C57BL/6 mice treated for 7 or 20 d with AT-ODN or CpG-ODN. Treatment duration correlated with malformation of splenic lymphoid follicles with enlarged B-cell zones upon CpG-ODN treatment, reduction of marginal zone B lymphocytes (B220 and CD21/35 stains), and damage and eventual disappearance of organized FDC-M1⁺ networks and PNA⁺ clusters. Metallophilic macrophage festoons were loosened and follicles were disrupted. *Tlr9*^{-/-} spleen morphology was unremarkable after 20 d of CpG-ODN. Scale bar, 200 μ m. **(b)** After 20 d of daily CpG-ODN treatment, almost all follicles disappeared, resulting in lack of discernible CD8⁺ T-cell zones compared with AT-ODN treatment. *Tlr9*^{-/-} mice showed normal organization and appearance of CD8⁺ T-cell zones. Scale bar, 200 μ m. **(c)** Morphometric analysis indicating numeric reduction of white-pulp follicles and FDC-M1⁺ and PNA⁺ clusters after 7 or 20 d of CpG-ODN treatment. *Tlr9*^{-/-} mice and AT-ODN-treated C57BL/6 mice had normal numbers of follicles and FDC-M1⁺ and PNA⁺ clusters. Error bars indicate s.d.; $n \geq 3$. **(d)** Quantification of relative spleen weights after 7 and 20 d of CpG-ODN treatment. *Ifnagr*^{-/-} mice showed almost normal relative spleen weights after CpG-ODN treatment.

that of lymphoid subpopulations was decreased. We detected a 2-fold relative decrease in B220⁺ B lymphocytes (Supplementary Fig. 2 online), a 3-fold decrease in CD138⁺B220⁺ plasma cells despite a 7.2-fold increase in absolute numbers, (Fig. 2f), a 4-fold decrease in CD21⁺CD35⁺IgMb⁺IgD⁻ marginal zone B lymphocytes (Fig. 2g) and a 4-fold decrease in IgMb^{int}IgD⁺ mature B

lymphocytes (Fig. 2h). CD4⁺ and CD8⁺ T cells were decreased 4-fold and 3-fold, respectively (Fig. 2d), and displayed a CD44^{hi}CD62L^{lo} activated phenotype (Fig. 2e and Supplementary Fig 2 online).

After ≥ 7 d, livers of CpG-ODN-treated wild-type mice showed multifocal infiltrates of B and T cells. Marked Kupffer cell hyper-

plasia expanded the sinusoids (Fig. 3a). Scattered hepatocellular degeneration, coalescing necrotic areas and regenerative nodules were apparent by 14 d (Supplementary Fig. 3 online). After 20 d, additional extramedullary hematopoiesis was observed (Supplementary Fig. 3 online). In contrast, *Tlr9*^{-/-} livers contained only rare small clusters of lymphocytes after 20 d of CpG-ODN treatment, similar to wild-type mice treated for 20 d with PBS or AT-ODN (Fig. 3b). Glutamate lactate dehydrogenase and alanine aminotransferase were markedly elevated in CpG-ODN-treated wild-type mice, whereas no increase was seen in AT-ODN treated mice or CpG-ODN treated *Tlr9*^{-/-} mice (Fig. 3c and data not shown). After ≥14 d of CpG-ODN treatment, wild-type (C57BL/6) mice developed 100- to 300- μ l hemorrhagic ascites containing primarily vacuolated macrophages, mesothelial cells, lymphocytes and rare neutrophils. There were no bacteria upon blood agar culture after 48 h.

IL-6, tumor necrosis factor (TNF) and interferon- γ (IFN- γ) increased substantially 2 h after injection of CpG-ODN, whereas IL-1 α was unaltered (Fig. 4a). Consequently, serum amyloid antecedent (SAA), which is induced by the above cytokines, showed an early and sustained increase in CpG-ODN-treated C57BL/6 mice¹³ but not in *Tlr9*^{-/-} mice (Fig. 4b).

CpG-ODN treatment (20 d) of mice lacking receptors for TNF (*Tnfr1*^{-/-})¹⁴ or type I (*Ifnar*^{-/-}) or type I/II (*Ifnagr*^{-/-}) interferons¹⁵ induced splenomegaly and lymphadenopathy and disturbed follicular microarchitecture, but to a lesser degree than in wild-type mice. AT-ODN treatment had no untoward effect (Supplementary Fig. 4 online). The SAA surge was not suppressed in *Tnfr1*^{-/-}, *Ifnar*^{-/-} or *Ifnagr*^{-/-} mice (Fig. 4b), perhaps because of signaling redundancy. C57BL/6 and *Tnfr1*^{-/-} mice developed hemorrhagic ascites, whereas AT-ODN-treated mice were normal.

129Sv mice proved much more sensitive to CpG-ODN than C57BL/6 mice. Two of three 129Sv mice developed splenomegaly, lymphadenopathy and hemorrhagic ascites requiring euthanasia by days 15–17. Spleens contained few follicles almost devoid of marginal zone and expanded B- and T-cell populations, and FDC networks were markedly decreased. In contrast, neither *Ifnar*^{-/-} nor *Ifnagr*^{-/-} mice developed ascites, and spleen weights of *Ifnagr*^{-/-} mice were almost normal (Fig. 1e). After 20 d of CpG-ODN treatment, *Ifnagr*^{-/-} spleen microarchitecture was only slightly disturbed (Supplementary Fig. 4 online) and marginal zone B-cell sheaths were almost unaltered, in contrast to their complete loss in 129Sv

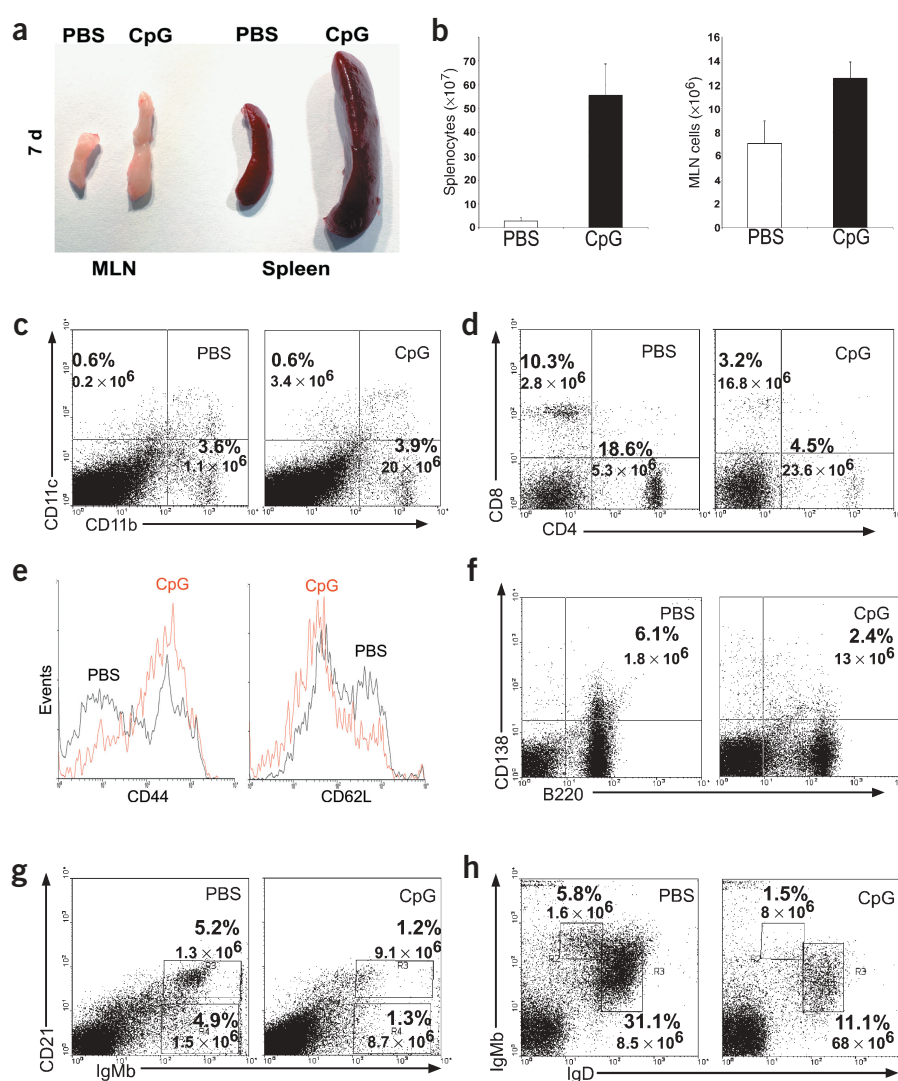


Figure 2 Quantitative effects of CpG-ODN on splenocyte subpopulations. (a) Sizes of mesenteric lymph nodes (MLN) and spleen were increased in CpG-ODN-treated mice compared with PBS-treated mice after 7 d of treatment. (b) Total cell numbers were increased in spleen (left) and mesenteric lymph nodes (right) of mice treated with CpG-ODN or PBS for 14 d. Error bars indicate s.d.; $n \geq 3$. (c, d) Fluorescence-activated cell sorting analysis of splenic CD11b⁺ macrophages and CD11c⁺ dendritic cells (c), and CD4⁺ and CD8⁺ T cells (d) after 14 d of treatment with PBS (left) or CpG-ODN (right). Absolute numbers of those cell populations and relative prevalence of macrophages and dendritic cells (as percentages) are shown. (e) After CpG-ODN treatment (red lines), splenic CD8⁺ (and CD4⁺; see Supplementary Fig. 2 online) T cells upregulated CD44 and downregulated CD62L, suggesting increased activation. Histograms were gated on CD8⁺ T cells. (f–h) Relative frequency of CD138⁺B220⁺ plasma cells was reduced despite an increase in absolute numbers. Similar changes were observed in CD21⁺CD35⁺IgM⁺ marginal zone B lymphocytes (gated on IgD⁻ lymphocytes) and transitional one-stage B cells (g), as well as IgM⁺IgD⁺ mature and transitional B lymphocytes (h).

and *Ifnar*^{-/-} mice. Repetitive treatment of wild-type mice with polyI:C, which induces IFN- α/β through TLR3 stimulation¹⁶, did not induce any derangement of lymphoid microarchitecture (data not shown).

129Sv mice (wild-type and *Ifnar*^{-/-}) suffered from extensive coalescing multifocal liver necrosis (data not shown). *Ifnagr*^{-/-} and *Tnfr1*^{-/-} livers exhibited little necrosis and much less inflammatory infiltration. CpG-ODN induced increased glutamate lactate dehydrogenase and alanine aminotransferase levels in wild-type mice, whereas no conspicuous changes were observed in *Tnfr1*^{-/-},

LETTERS

Ifnar^{-/-} and *Ifnagr*^{-/-} mice (Fig. 3c). Thus, interferons and, to a lesser degree, TNF contribute to TLR9-dependent CpG-ODN hepatotoxicity. However, all CpG-ODN-treated mice (except *Ifnagr*^{-/-}) showed thrombocytopenia and slightly reduced hematocrit (Fig. 3d). No liver lesions developed in polyI:C-treated mice.

We then tested whether CpG-ODN can induce antibodies to prion protein (PrP). Three weeks after a 20-d treatment with CpG-ODN (started 7 h after intraperitoneal inoculation of 5log (half-maximal lethal dose) scrapie prions³), PrP-specific antibody titers in wild-type (C57BL/6) mice did not exceed background levels (<1:20, *n* = 3; Fig. 4c) whereas PrP-deficient (*Prnp*^{-/-}) mice immunized with a recombinant PrP-PrP fusion molecule¹⁷ had a titer of 1:82,000. Thus, the antiprion effect of CpG-ODN is not due to PrP-specific antibody responses.

Mice were then immunized intravenously with 2×10^8 plaque-forming units (PFU) of ultraviolet-inactivated (to avoid cytokine effects on viral replication) vesicular stomatitis virus (UV-VSV) after 7 or 14 d of treatment with CpG-ODN or PBS. VSV-neutralizing IgM titers were reduced and immunoglobulin class switching was suppressed (Fig. 4d) in CpG-ODN treated wild-type mice, but not in *Tlr9*^{-/-} mice (data not shown). Challenge with a range of UV-VSV doses (8×10^8 and 5×10^7 PFU) revealed that this effect is dose dependent (data not shown).

By expanding lymphoid B-cell pools, CpG-ODN treatment may augment natural neutralizing antibodies¹⁸, which may quench the UV-VSV inoculum. However, serum IgM, IgG1, IgG2a and IgG2b and VSV-specific natural antibody titers did not differ between mice treated for 7 d with CpG-ODN and PBS-treated controls (*n* = 3; data not shown).

Wild-type mice were also treated with CpG-ODN or AT-ODN for 14 d, then challenged subcutaneously with 50 μg keyhole limpet hemocyanin (KLH) in complete Freund adjuvant (CFA). Antibody responses to KLH were reduced until day 30, but then slowly recovered (*n* = 3; data not shown), perhaps because antigen was slowly released from its local depot after cessation of CpG-ODN treatment, or because of differential sensitivity of the various routes of delivery to lymphoid follicle disruption.

Many studies indicate that CpG-ODN are immunostimulatory, but in most of those cases only one or two doses of CpG-ODN were injected^{19,20}. Upon repetitive administration, we observed lymphoid microarchitectural damage proportional to the duration of treatment. As a functional correlate, adaptive B-cell immune responses became profoundly impaired. Treatment for ≥ 14 d elicited grave systemic toxicity, including peritonitis, hepatotoxicity, ascites and thrombocytopenia. All effects were strictly dependent on the presence of CpG sequences in the oligonucleotides and on host expression of TLR9. We conclude that immune stimulation and untoward effects of CpG-ODN are elicited through similar molecular pathways.

Hepatotoxicity and splenomegaly were partially counteracted by ablation of IFN and, to a lesser extent, TNF signaling. Lack of IFN- α receptor (IFN- α R), or both IFN- α R and IFN- γ R, also reduced destruction of lymphoid follicles by CpG-ODN (Supplementary Fig. 4 online). Conversely, chronic IFN induction by the TLR3 agonist polyI:C was neither lymphoclastic nor hepatotoxic. This suggests that the effector pathways are pleiotropic and redundant, with IFN and TNF contributing to the immunotoxic and hepatotoxic effects of CpG-ODN. Intriguingly, these

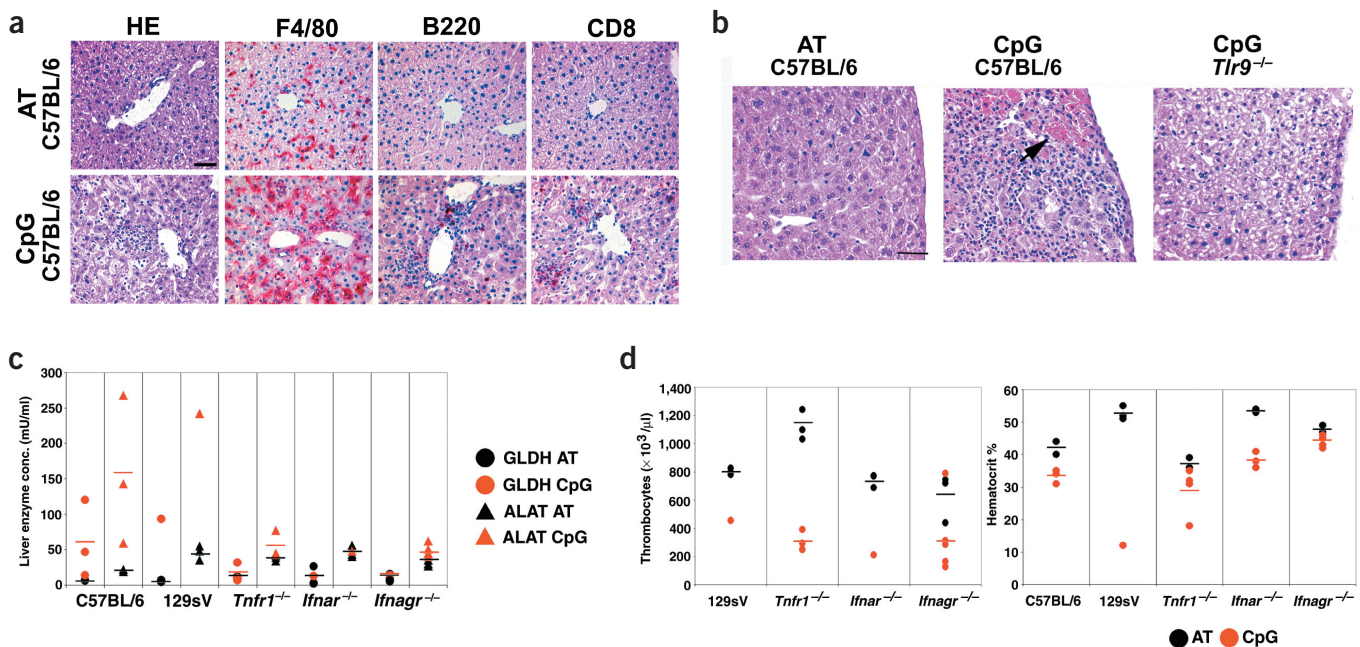


Figure 3 Hepatotoxicity of CpG-ODN. (a) Liver after 7 d of CpG-ODN treatment, revealing extensive hyperplasia of F4/80⁺ Kupffer cells lining sinusoids and patchy infiltrates of B220⁺ and CD8⁺ cells. Few scattered CD4⁺ cells were detected. Scale bar, 50 μm. (b) H&E-stained paraffin sections of C57BL/6 and *Tlr9*^{-/-} livers after 20 d of CpG-ODN or AT-ODN treatment. Areas of hepatocellular degeneration and necrosis (arrow) ranging from single cells to coalescing foci with erythrocytes, fibrin, leukocytes and reactive mesothelial cells. Scale bar, 50 μm. (c) Elevation of liver-specific serum enzymes glutamate lactate dehydrogenase (GLDH) and alanine aminotransferase (ALAT) in wild-type mice after 20 d of treatment (*n* = 3 per group). None of the receptor-deficient genotypes analyzed (*Tnfr1*^{-/-}, *Ifnar*^{-/-} and *Ifnagr*^{-/-}) showed a conspicuous increase. (d) Thrombocytes were markedly depleted in peripheral blood after 20 d of CpG-ODN treatment, in all groups analyzed (left). Hematocrit values were analyzed in peripheral blood after 20 d of CpG-ODN or AT-ODN treatment (right).

morphological and functional effects are similar to those described after lymphocytic choriomeningitis virus infection²¹, which are dependent on CD8⁺ T cells, IFN and TNF^{21–23}.

How can these findings be reconciled with the immunostimulatory properties of CpG-ODN? We observed an increase in absolute CD4⁺ and CD8⁺ T-cell numbers, as described earlier^{12,24}. However, primary B-lymphocyte responses against viruses rely on intact marginal zone macrophages for uptake of viral particles, and on marginal zone B cells for the induction of early IgM²⁵, whereas class switching and secondary immune responses correlate with FDC networks in germinal centers^{18,26}. All of these structures were depleted in CpG-ODN-treated mice. Absolute numbers of CD4⁺, CD8⁺ and B220⁺ cells increased during CpG-ODN treatment, yet their density was reduced because of much stronger expansion of myeloid and erythroid compartments. This may contribute to immunosuppression by diluting immune cells and lowering the probability of their productive encounters.

Mice on a 20-d CpG-ODN regimen showed prolonged survival after prion inoculation³. Because prion infection after CpG-ODN treatment did not induce PrP-specific antibodies, antiprion protection may be a consequence of follicle destruction. Germinal centers are the major site of peripheral prion amplification, and their genetic⁴ or pharmacological⁹ disruption abrogates susceptibility to peripherally administered prions. Accordingly, antiprion efficacy³, follicle disruption and immunosuppression were correlated with the duration of CpG-ODN treatment.

CpG-ODN is entering clinical trials for several applications, including cancer immunotherapy, allergen immunotherapy and antimicrobial vaccination. For most such applications, CpG-ODN is used as an adjuvant once or in broadly spaced doses, rather than daily, and alternative formulation linking CpG-ODN and antigen may be applicable²⁷. In addition, TLR9 expression may be lower in human macrophages than in mouse macrophages. For antiprion postexposure prophylaxis in humans, repeated systemic administration of high doses of CpG-ODN has been advocated³. The present findings may limit the feasibility of such regimens; instead, antiprion prophylaxis is likely to require specific targeting of the cells responsible for prion amplification and neuroinvasion.

METHODS

CpG-ODN and AT-ODN treatment. Mice were maintained under specific pathogen-free conditions. Age- and sex-matched C57BL/6 mice (8–14 weeks) were injected daily for 2, 7, 14 or 20 d with 10 nmol (60 µg/mouse) CpG-ODN 1826 or AT-ODN (5'-GCTTGATGACTCAGCCGAA-3'), with polyI:C (50 µg/mouse) or with PBS intraperitoneally (30 µl/injection). One group of mice was inoculated intraperitoneally with RML 5.0 scrapie prions 7 h before starting a 20-d regimen of CpG-ODN treatment, as previously published³. Mice were killed 24 h after the last injection. Splenic, lymph nodal and liver samples were stored in HBSS and immediately

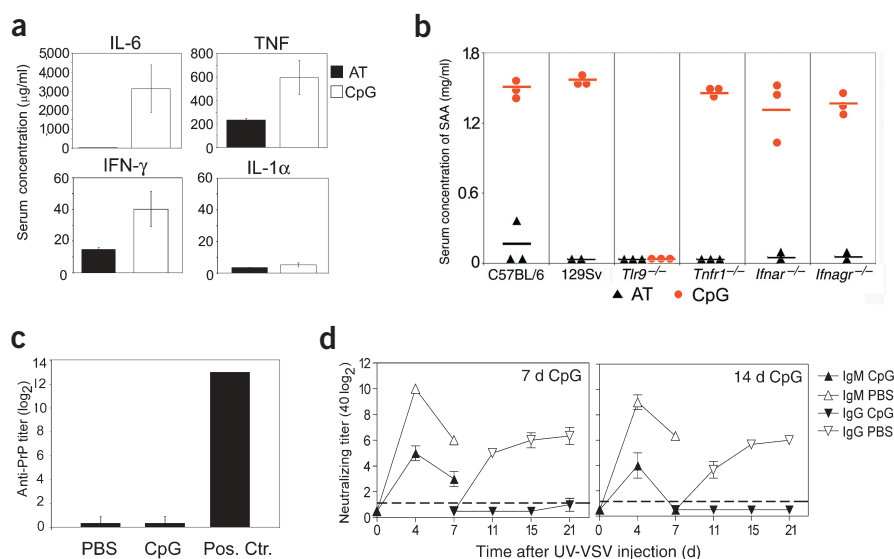


Figure 4 Attenuation of immunoglobulin class switching and absence of humoral immunity to PrP. (a) Early inflammatory cytokines in sera of CpG-ODN treated mice, 2 h after injection ($n = 3$ mice per group, analyzed in duplicate). (b) Induction of acute phase protein SAA in sera of CpG-ODN-, AT-ODN- or AT/PBS-treated mice (day 10 of 20-d regimen). Various wild-type (C57BL/6 and 129Sv) and receptor-deficient ($Tnfr1^{-/-}$, $Tlr9^{-/-}$, $Ifnar^{-/-}$ and $Ifnagr^{-/-}$) genotypes were analyzed. SAA increased markedly in all CpG-ODN-treated mice except $Tlr9^{-/-}$ ($n = 3$). (c) PrP-specific antibody titers, measured by ELISA 40 d after prion inoculation and 20 d after daily treatment with CpG-ODN. No titer was detected in mice treated with CpG-ODN or PBS. $Prnp^{-/-}$ mice immunized with recombinant PrP-PrP fusion protein showed high antibody titers (Pos. Ctr.). (d) Neutralizing IgM and IgG titers after 7 d (left) or 14 d (right) of PBS or CpG-ODN treatment and subsequent immunization with UV-VSV. PBS-treated mice showed class switching from IgM to IgG between days 7 and 11 after immunization. CpG-ODN-treated mice showed lower titers of IgM on day 4 after UV-VSV challenge, and showed a marked reduction in class switching, with very low titers 21 d after challenge. Dotted lines indicate detection limit of assay. Error bars in a, c, d indicate s.d.; $n \geq 3$.

frozen in isopentane and liquid nitrogen for histological analysis, or fixed in 4% paraformaldehyde at room temperature. All manipulations were approved by the Cantonal Animal Experimentation Committee.

Histology and immunohistochemistry. Paraffin-fixed (6 µm) and consecutively frozen (5 or 10 µm) sections of spleen, mesenteric lymph nodes, inguinal lymph nodes or liver were stained with H&E. Antibodies FDC-M1 (4C11; 1:50; Becton Dickinson) and CD21/35 (8C12; 1:100; PharMingen), and antibodies to CD45RO/B220 (RA3-6B2; 1:400; PharMingen), MOMA-1 (1:50; BMA; Augst), pan-cytokeratin (Lu5; 1:200; BMA; Augst, Switzerland), F4/80 (1:50; Serotec) and PNA (1:100; Vector), were used as primary reagents for immunohistochemistry and lectin histochemistry as described²⁸. Morphometric analysis was done as described²⁹. Numbers were normalized to numbers per 10 mm² of spleen section.

Viruses. The Indiana strain of VSV (VSV-IND; Mudd-Summers isolate) was originally obtained from D. Kolakofsky (University of Geneva, Switzerland). VSV-IND was propagated on BHK-21 cells and plaqued on Vero cells. For experiments, VSV-IND was ultraviolet-inactivated (7UV 15W, Philips) for 5 min in a thin layer of liquid in a 60-mm Petri dish.

VSV-specific serum neutralization test. Neutralizing antibody titers of sera were determined as described^{22,23}. Sera were prediluted 40-fold in supplemented MEM and heat-inactivated for 30 min at 56 °C. Serial 2-fold dilutions of sera were mixed with equal volumes of virus diluted to contain 500 PFU/ml. The mixture was incubated for 90 min at 37 °C in an atmosphere containing 5% CO₂. The serum-virus mixture (100 µl) was transferred onto Vero cell monolayers in 96-well plates and incubated for 1 h at 37 °C. Monolayers were overlaid with 100 µl DMEM containing 1%

methylcellulose. After incubation for 24 h at 37 °C, the overlay was removed and the monolayer was fixed and stained with 0.5% crystal violet. The highest dilution of serum that reduced the number of plaques by 50% was taken as the neutralizing titer. To determine IgG titers, and because second-stage antibodies cannot be detected in neutralization assays, undiluted serum was pretreated with an equal volume of 0.1 M β -mercaptoethanol in saline^{22,23}.

PrP-specific antibody titer determinations. ELISA for PrP-specific antibodies was done as described³⁰. Plates were coated with 5 μ g/ml of recombinant mouse PrP, washed with PBST and blocked with 5% BSA. After washing, plates were incubated with 30 μ l of twofold serially diluted serum (1:20 prediluted) in PBST containing 1% BSA, then probed with horseradish peroxidase-conjugated rabbit antibody to mouse IgG/IgA/IgM (H+L; 1:1,000 dilution; Zymed Laboratories). Plates were developed with ABTS and optical density was measured at 405 nm. Titer was defined as the highest dilution with optical density greater than twice that of the technical background, which was calculated as the average of uncoated wells and those incubated without the serum. As a positive control, we used serum of *Prnp*^{-/-} mice immunized with a recombinant PrP-PrP fusion molecule, measured on day 27 of immunization¹⁷.

Measurement of serum cytokines and SAA. Mouse blood was collected 2 h after CpG-ODN injection into serum separator microtubes, and centrifuged for 10 min at 5,400 g to obtain serum. IL-1 α , IL-6, IFN- γ and TNF concentrations were measured by ELISA. For IL-1 α , IL-6 and TNF, ELISA kits were used according to the manufacturer's instructions (BD Biosciences, catalog nos. 550347, 555240 and 555268, respectively). For IFN- γ determination, antibodies (R&D Biosystems) were used for capture and detection according to the manufacturer's instructions (capture antibody, MAB785; detection antibody, BAF 485). SAA levels were determined in 100 \times prediluted serum, by ELISA, using a commercially available kit (Biosource, catalog no. KMA 0012) following the manufacturer's instructions.

KLH/CFA immunization. Mice were treated for 14 d with CpG-ODN or AT-ODN, and subcutaneously injected on day 15 with 50 μ g KLH (Sigma, catalog no. H7017) emulsified in CFA (Sigma, catalog no. F5881). Mice were bled on days 7, 14, 21 and 28 after KLH/CFA injection. For detection of KLH-specific IgG antibody titers, ELISA plates were coated overnight at 4 °C with 2.5 μ g/ml of recombinant KLH (Sigma, catalog no. H7017). Plates were washed with PBST and blocked with 10% BSA for 2 h at room temperature. After washing, plates were incubated with 30 μ l of twofold serially diluted serum (1:40 prediluted) in blocking buffer, and probed with horseradish peroxidase-conjugated goat antibody to mouse IgG γ (1:1,000 dilution; Zymed Laboratories). Plates were developed with ABTS and optical density was measured at 405 nm. Titer was defined as the dilution of the turning point (half-maximal optical density); the technical background was calculated as the average of uncoated wells and wells incubated without the serum.

Note: Supplementary information is available on the Nature Medicine website.

ACKNOWLEDGMENTS

We thank B. Odermatt, B. Padberg and P. Schwarz for help. This work is supported by grants of the Bundesamt für Bildung und Wissenschaft (EU) and the Swiss National Foundation to A.A. and R.Z., the US National Prion Research Program to A.A. and C.S., and the National Centre of Competence in Research on neural plasticity and repair to A.A. M.H. is supported by a generous educational grant from the Catello family and by the Verein zur Förderung des Akademischen Nachwuchses. M.P. was supported by a Ph.D. fellowship from the Zentrum für Neurowissenschaften Zürich and a scientific grant from the United Banks of Switzerland. C.S. was supported by National Institutes of Health grant K08-AI01802.

COMPETING INTERESTS STATEMENT

The authors declare that they have no competing financial interests.

Received 24 November 2003; accepted 2 January 2004
Published online at <http://www.nature.com/naturemedicine/>

- Krieg, A.M. CpG motifs in bacterial DNA and their immune effects. *Annu. Rev. Immunol.* **20**, 709–760 (2002).
- Hemmi, H. *et al.* A Toll-like receptor recognizes bacterial DNA. *Nature* **408**, 740–745 (2000).
- Sethi, S., Lipford, G., Wagner, H. & Kretzschmar, H. Postexposure prophylaxis against prion disease with a stimulator of innate immunity. *Lancet* **360**, 229–230 (2002).
- Klein, M.A. *et al.* A crucial role for B cells in neuroinvasive scrapie. *Nature* **390**, 687–690 (1997).
- Aucouturier, P. *et al.* Infected splenic dendritic cells are sufficient for prion transmission to the CNS in mouse scrapie. *J. Clin. Invest.* **108**, 703–708 (2001).
- Adachi, O. *et al.* Targeted disruption of the MyD88 gene results in loss of IL-1- and IL-18-mediated function. *Immunity* **9**, 143–150 (1998).
- Hacker, H. *et al.* Immune cell activation by bacterial CpG-DNA through myeloid differentiation marker 88 and tumor necrosis factor receptor-associated factor (TRAF)6. *J. Exp. Med.* **192**, 595–600 (2000).
- Prinz, M. *et al.* Prion pathogenesis in the absence of Toll-like receptor signalling. *EMBO Rep.* **4**, 195–199 (2003).
- Montrasio, F. *et al.* Impaired prion replication in spleens of mice lacking functional follicular dendritic cells. *Science* **288**, 1257–1259 (2000).
- Aguzzi, A., Montrasio, F. & Kaeser, P.S. Prions: health scare and biological challenge. *Nat. Rev. Mol. Cell. Biol.* **2**, 118–126 (2001).
- Sparwasser, T. *et al.* Immunostimulatory CpG-oligodeoxynucleotides cause extramedullary murine hemopoiesis. *J. Immunol.* **162**, 2368–2374 (1999).
- Davila, E., Velez, M.G., Heppelmann, C.J. & Celis, E. Creating space: an antigen-independent, CpG-induced peripheral expansion of naive and memory T lymphocytes in a full T-cell compartment. *Blood* **100**, 2537–2545 (2002).
- Schmidt, U., Wagner, H. & Miethke, T. CpG-DNA upregulates the major acute-phase proteins SAA and SAP. *Cell. Microbiol.* **1**, 61–67 (1999).
- Rothe, J. *et al.* Mice lacking the tumour necrosis factor receptor 1 are resistant to TNF-mediated toxicity but highly susceptible to infection by *Listeria monocytogenes*. *Nature* **364**, 798–802 (1993).
- Muller, U. *et al.* Functional role of type I and type II interferons in antiviral defense. *Science* **264**, 1918–1921 (1994).
- Alexopoulou, L., Holt, A.C., Medzhitov, R. & Flavell, R.A. Recognition of double-stranded RNA and activation of NF- κ B by Toll-like receptor 3. *Nature* **413**, 732–738 (2001).
- Gilch, S. *et al.* Polyclonal anti-PrP auto-antibodies induced with dimeric PrP interfere efficiently with PrPSc propagation in prion-infected cells. *J. Biol. Chem.* **278**, 18524–18531 (2003).
- Ochsenbein, A.F. *et al.* Control of early viral and bacterial distribution and disease by natural antibodies. *Science* **286**, 2156–2159 (1999).
- Oxenius, A., Martinic, M.M., Hengartner, H. & Klenerman, P. CpG-containing oligonucleotides are efficient adjuvants for induction of protective antiviral immune responses with T-cell peptide vaccines. *J. Virol.* **73**, 4120–4126 (1999).
- Vabulas, R.M., Pircher, H., Lipford, G.B., Hacker, H. & Wagner, H. CpG-DNA activates *in vivo* T cell epitope presenting dendritic cells to trigger protective antiviral cytotoxic T cell responses. *J. Immunol.* **164**, 2372–2378 (2000).
- Binder, D., Fehr, J., Hengartner, H. & Zinkernagel, R.M. Virus-induced transient bone marrow aplasia: major role of interferon- α/β during acute infection with the noncytopathic lymphocytic choriomeningitis virus. *J. Exp. Med.* **185**, 517–530 (1997).
- Riviere, Y., Gresser, I., Guillon, J.C. & Tovey, M.G. Inhibition by anti-interferon serum of lymphocytic choriomeningitis virus disease in suckling mice. *Proc. Natl. Acad. Sci. USA* **74**, 2135–2139 (1977).
- Odermatt, B., Eppler, M., Leist, T.P., Hengartner, H. & Zinkernagel, R.M. Virus-triggered acquired immunodeficiency by cytotoxic T-cell-dependent destruction of antigen-presenting cells and lymph follicle structure. *Proc. Natl. Acad. Sci. USA* **88**, 8252–8256 (1991).
- Davila, E. & Celis, E. Repeated administration of cytosine-phosphorothiolated guanine-containing oligonucleotides together with peptide/protein immunization results in enhanced CTL responses with anti-tumor activity. *J. Immunol.* **165**, 539–547 (2000).
- Martin, F., Oliver, A.M. & Kearney, J.F. Marginal zone and B1 B cells unite in the early response against T-independent blood-borne particulate antigens. *Immunity* **14**, 617–629 (2001).
- Fehr, T. *et al.* Correlation of anti-viral B cell responses and splenic morphology with expression of B cell-specific molecules. *Int. Immunol.* **12**, 1275–1284 (2000).
- Storni, T. *et al.* Critical role for activation of antigen-presenting cells in priming of cytotoxic T cell responses after vaccination with virus-like particles. *J. Immunol.* **168**, 2880–2886 (2002).
- Karrer, U. *et al.* Antiviral B cell memory in the absence of mature follicular dendritic cell networks and classical germinal centers in TNFR1^{-/-} mice. *J. Immunol.* **164**, 768–778 (2000).
- Prinz, M. *et al.* Positioning of follicular dendritic cells within the spleen controls prion neuroinvasion. *Nature* **425**, 957–962 (2003).
- Heppner, F.L. *et al.* Prevention of scrapie pathogenesis by transgenic expression of anti-prion protein antibodies. *Science* **294**, 178–182 (2001).